Auton Robot (2006) 21:79–97
DOI 10.1007/s10514-006-7806-4

High accuracy path tracking for vehicles in presence of sliding: Application to farm vehicle automatic guidance for agricultural tasks

Roland Lenain · Benoit Thuilot · Christophe Cariou · Philippe Martinet

Published online: 12 June 2006

Abstract. When designing an accurate automated guidance system for vehicles, a major problem is sliding and pseudo-sliding effects. This is especially the case in agricultural applications, where five-centimetre accuracy with respect to the desired trajectory is required, although the vehicles are moving on slippery ground.

It has been established that RTK GPS was a very suitable sensor to achieve automated guidance with such high precision: several control laws have been designed for vehicles equipped with this sensor, and provide the expected guidance accuracy as long as the vehicles do not slide. In previous work, further control developments have been proposed to take sliding into account: guidance accuracy in slippery environments has been shown to be preserved, except transiently at the beginning/end of curves. In this paper, the design of this control law is first recalled and discussed. A Model Predictive Control method is then applied in order to preserve accuracy of guidance even during these curvature transitions. Finally, the overall control scheme is implemented, and improvements with respect to previous guidance laws are demonstrated through full-scale experiments.

Keywords Non linear control · Adaptive control · Model Predictive Control of vehicles · Vehicle motion in presence of sliding effects · Automated guided vehicle · Path tracking of mobile robot · Agricultural robots and environmental applications

R. Lenain (✉) · C. Cariou
Cemagref, 24 av. des Landais BP50085, 63172 Aubière Cedex, France
e-mail: roland.lenain@cemagref.fr

C. Cariou
e-mail: christophe.cariou@cemagref.fr

B. Thuilot · P. Martinet
LASMEA, 24 av. des Landais,
63177 Aubière Cedex, France

B. Thuilot
e-mail: benoit.thuilot@lasmea.univ-bpclermont.fr

P. Martinet
e-mail: philippe.martinet@lasmea.univ-bpclermont.fr

1. Introduction

Environmental problems are steadily gaining importance in the political stakes of industrialized countries, especially with respect to agricultural activities. In particular, one way to be more environmentally friendly is to design automatic systems for farm vehicle guidance. Such developments can increase the accuracy of a task during long periods of work, and hence reduce negative impacts on the environment linked to agronomic activities. For example, when using an automated guidance device, spraying can be achieved more accurately, so that areas with too much fertilizer can be reduced. Pollution and the time needed to perform farming tasks are then both reduced. Furthermore, such automation can improve the farmer's comfort, as the tracking task is performed by the vehicle itself. The driver can then focus on the work done by the implement fitted and stay concentrated all day long. This positive aspect, added to the capacity of guidance laws developed to detect cases which could be dangerous, increases security with respect to farm applications. Environmental considerations, benefits to yield and security improvement generate a lot of interest both from farmers and manufacturers. For this reason, the latter have developed various solutions for automated path following during the

last few years. As an example, research work described in this paper is conducted in partnership with the agricultural machine manufacturer CLAAS.

Numerous systems have already been marketed for different applications, using various technologies and supplying more or less accuracy. Some of them use relative sensors such as the device dedicated to harvesting machines marketed by manufacturer CLAAS, relying on laser technology (see (Brunnert, 2003)), or such as research work carried out at Cemagref using artificial vision (see (Debain et al., 2000)). However, most current developments focus on Global Positioning Systems (GPS), whose accuracy is becoming better and better. Centimetre accuracy can now be achieved with the Real-Time Kinematic version (RTK-GPS). Early devices marketed have used GPS in addition to other sensors (such as the Fiber Optic Gyroscope in Nagasaka et al. (1997), vision in Reid and Niebuhr (2001) or several GPS antennas in O'Connor et al. (1996)). The latest solutions are based on the use of a single GPS or RTK-GPS sensor (e.g. Trimble systems or the Outback guidance system, which proposes a complete panel of GPS guidance solutions). However, acceptable accuracy with respect to agricultural tasks can be attained only when following straight lines on level ground.

Previous research work on RTK-GPS based guidance systems (detailed in Thuilot et al. (2002) and in Cordesses (2001)) has investigated not only straight line but also curved path tracking and has proposed control solutions offering very good accuracy (about 10 cm) whatever the path to be followed. Unfortunately, this accuracy is seriously impaired as soon as the vehicles slide, which inevitably occurs during agricultural tasks (curved path tracking on slippery fields or guidance on sloping ones). There are currently a few programmes devoted to vehicle control in the presence of sliding (see e.g. (Ellouze and Andréa-Novel, 2000)). However, they are always dedicated to steering road vehicles outside the sliding domain (their aim is to ensure that, as far as possible, vehicles satisfy conditions of pure rolling without sliding). Moreover, they use dynamic models whose parameters could hardly be estimated on-line in agricultural applications: complex and expensive measurement devices would be required, and estimation of parameters would be very sensitive to disturbances (such models are indeed mainly dedicated to cars). Another field of research which deals with the problem of sliding is localization. In this case, detection of sliding is important to preserve good estimation of the robot's position, whatever its path may be. Sliding has then to be integrated into the localization algorithm as is done in Lindgren et al. (2002), for example). However the approaches developed are specific to localization and cannot be easily transposed to address control problems.

In this paper, good estimation of vehicle position is available, relying on an RTK-GPS sensor. The occurrence of sliding, and the effects associated with such a phenomenon, have to be evaluated on-line so that they can be introduced into the control laws to be designed, which can prevent vehicles from making the lateral deviations generally observed in the presence of sliding. In the first part, an extended kinematic model accounting for sliding effects is designed. It enables the characterization of vehicle behaviour with respect to our measurement system. A complete dynamic model, such as that used in Ellouze and Andréa-Novel (2000), has not been considered, because it is hardly applicable for control design. The validity of the extended kinematic model is checked theoretically and experimentally. Next, a new control law is designed in order to correct vehicle behaviour in the presence of sliding. Preliminary tests are presented. Satisfactory performance can be observed, except at transitions in sliding conditions (when sliding appears or disappears). Further control developments, relying on a Model Predictive Control approach, are then introduced to deal with these limitations. Finally, full scale experiments are reported and show the improvements achieved when the sliding phenomenon is thus taken into account, with respect to applications demanding high accuracy path tracking capabilities on natural ground.

2. Work context and previous work

2.1. Experimental background

Since the work described in this paper is carried out in partnership with German manufacturer CLAAS, the automatic guidance developments have to be experimentally validated on several actual vehicles. Figure 1 shows the experimental vehicles lent by CLAAS: an Ares 640 tractor and a Dominator combine harvester.

All the experiments reported in this paper were carried out with the tractor and the description of the control laws is relevant to the case of the tractor. To address the case of the combine harvester, since the steering axle is the rear one, sign modifications have to be introduced. However, the control principles and performance are identical.

Fig. 1 Vehicles used in actual experiments

These experimental vehicles are the same as those sold to customers, except that an actuator has been introduced to steer the front wheels and an RTK-GPS sensor has been added to provide vehicle localization.

Specifically, the RTK GPS sensor is an Aquarius 5002 unit manufactured by Thales Navigation. It supplies a positioning signal accurate to within 2 cm, at a 10 Hz sampling frequency. This sensor is composed of a reference antenna and a mobile antenna fixed on the vehicle. For the tractor, the mobile antenna is fitted on the top of the cabin, straight up above the centre of the rear axle (since this is the vehicle point to be controlled, as described in Section 2.2.1). This location ensures satisfactory satellite reception, but position measurement is then sensitive to cabin oscillations. On level fields, few oscillations are indeed observed, since the cabin is linked to the axle via shock absorbers and an anti-roll bar. The only unfavourable case is sloping fields, since the shock absorbers on one side of the vehicle are then more compressed than the ones on the other side, thus generating noticeable cabin oscillations. However, although these movements add some noise to the position measurement, they do not lead to a bias in tracking error results, as will be explained in greater detail in Section 2.2.4.

In all the experiments reported in this paper, vehicle velocity has always been manually controlled by the driver. Thus the only control variable is the steering angle. A nested closed loop scheme with two levels is currently implemented on the tractor. In this paper, only the higher level closed loop is discussed: from the localization measurement supplied by the RTK-GPS sensor, the control laws to be designed aim at providing the steering angle value to be sent to the steering actuator. An inner closed loop, making use of an angular sensor located on the front right wheel, thus ensures that the actual steering angle converges with the desired angle.

2.2. Control assuming rolling without sliding

2.2.1. Modelling

Since the extended kinematic model is derived from the classical model relying on conditions of rolling without sliding, the latter, known as the Ackermann model, is recalled here. As shown in Fig. 2, the vehicle is reduced to a bicycle shape: the front axle (or respectively the rear axle), actually composed of two wheels, is considered as a single wheel. As the goal of the application is trajectory tracking, the description of the vehicle's movement is made with respect to the path to be followed, assumed to be known in our application (preliminarily computed or stored from a previous run). Specifically, the absolute state of the vehicle (absolute location and heading, supplied by the RTK GPS sensor) is converted into a relative state (curvilinear abscissa, lateral deviation and heading deviation). The parameters and notations used in this model are listed below:

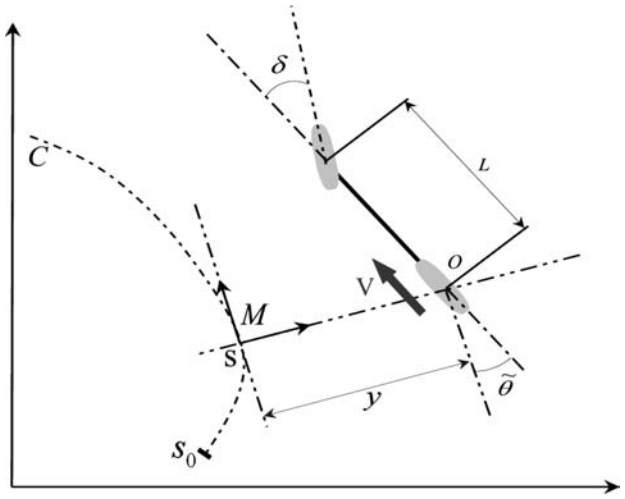

Fig. 2 Classical kinematic model parameters

- $\mathcal{C}$ is the path to be followed.
- O is the centre of the vehicle's virtual rear wheel. This is the point to be explicitly controlled.
- M is the point on $\mathcal{C}$ which is the closest to O. M is assumed to be unique, which is realistic when the vehicle remains quite close to $\mathcal{C}$.
- s is the curvilinear coordinate of point M along $\mathcal{C}$. $c(s)$ denotes the curvature of $\mathcal{C}$ at that point.
- y and $\tilde{\theta}$ are respectively the lateral and angular deviation of the vehicle with respect to the reference path $\mathcal{C}$ (see Fig. 2).
- δ is the virtual front wheel steering angle and the sole control variable.
- v is the vehicle's linear velocity, considered here as a parameter, whose value may be time-varying during the travel of the vehicle.
- L is the vehicle wheelbase.

With these notations, and assuming in this case that the two virtual wheels (front and rear) of the vehicle satisfy conditions of rolling without sliding, classical system (1) can be calculated (for further details, see (Thuilot et al., 2002)):

$$\begin{cases} \dot{s} = \dfrac{v\cos\tilde{\theta}}{1-c(s)y} \\ \dot{y} = v\sin\tilde{\theta} \\ \dot{\tilde{\theta}} = v\left[\dfrac{\tan\delta}{L} - \dfrac{c(s)\cos\tilde{\theta}}{1-c(s)\,y}\right] \end{cases} \tag{1}$$

The only singularity of model (1) is $(1 - c(s)\,y) = 0$, which occurs only if point O is superposed on the curvature centre of reference path $\mathcal{C}$. From a practical point of view, the curvature of reference paths is never very large, so

that, if point O is reasonably close to $\mathcal{C}$, the singularity is never met.

2.2.2. *Control law without sliding accounted*

The objective of curved path following is to ensure the convergence of y and $\tilde{\theta}$ towards 0, independently of changes in the variable s (which mainly depends on the value of parameter v). The control approach proposed in Thuilot et al. (2002) consists in pointing out that a part of non-linear model (1) can be converted, *without any approximation*, into linear equations. More precisely, injecting into model (1) the invertible non-linear state transformation:

$$\Theta((s,\, y,\, \tilde{\theta})) = (a_1, a_2, a_3) \stackrel{\Delta}{=} (s,\, y,\, (1 - c(s)\, y) \tan\tilde{\theta}) \qquad (2)$$

and describing the vehicle's movement with respect to s (instead of with respect to time) leads to the linear model:

$$\begin{cases} \dfrac{d\, a_2}{d\, s} = a_3 \\ \dfrac{d\, a_3}{d\, s} = m_3 \end{cases} \qquad (3)$$

Computations show that the new control variable m_3 and the actual control variable δ are related by an invertible transformation. Such a model conversion can be achieved, since model (1) enters into the class of non-linear systems which can be converted into chained forms (see for instance (Samson, 1995)).

The celebrated linear control theory can then be used to design control law m_3 in order to ensure the convergence of $(a_2,\, a_3)$ to 0. In view of (2), this consequently implies the desired convergence of $(y,\, \tilde{\theta})$ to 0. If m_3 is chosen as a classical PD controller, the inversion of the non-linear relation between m_3 and δ (see (Thuilot et al., 2002)) gives the non-linear control law to be eventually implemented:

$$\begin{aligned} \delta(y, \tilde{\theta}) = \arctan\Bigg(L \Bigg[\frac{cos^3\tilde{\theta}}{(1 - c(s)y)^2} \Bigg(\frac{d\, c(s)}{d\, s} y \tan\tilde{\theta} \\ - \; K_d (1 - c(s)\, y) \tan\tilde{\theta} - K_p\, y \\ + \; c(s)\big(1 - c(s)\, y\big) \tan^2\tilde{\theta}\big) + \frac{c(s) \cos\tilde{\theta}}{1 - c(s)y} \Bigg] \Bigg) \end{aligned} \qquad (4)$$

Since control law (4) is designed from system (3), which is driven with respect to curvilinear abscissa, its capabilities are independent of vehicle velocity. To be precise, closed loop performance can be adjusted by tuning parameters $(K_p,\, K_d)$, which here define a distance of convergence.

The implementation of control law (4) requires the on-line measurement of the vehicle state vector $(s,\, y,\, \tilde{\theta})$. The first two elements s and y can be calculated straightforwardly from the absolute coordinates of O, supplied by the RTK GPS sensor, and from the reference path $\mathcal{C}$. In contrast, no sensor is available to provide a direct measurement of vehicle heading. The last element of the vehicle state vector has then to be reconstructed. A Kalman filter based on model (1), and making use of the vehicle velocity vector supplied by the RTK GPS sensor, has been designed. The angular deviation $\tilde{\theta}$ is then obtained by using the direction of the tangent to the reference path $\mathcal{C}$ at point M.

2.2.3. *Experimental results*

Since control law (4) was designed on the assumption of rolling without sliding, trajectory tracking is actually achieved with satisfactory accuracy as long as the sliding phenomenon is negligible (i.e. when tracking reference paths with a very low curvature on level ground). But as soon as sliding appears (e.g. when tracking curved paths on level ground or straight lines on sloping fields), guidance accuracy is impaired and no longer meets the expectations of agricultural applications.

To illustrate this point, the reference path shown in Fig. 3 was tracked, relying on control law (4). This reference path, composed of two straight lines linked by a half-turn, was recorded when the tractor was manually driven on an actual field (slippery ground).

Figure 4 shows the lateral deviation y (i.e. the tracking error) with respect to the curvilinear abscissa s travelled along the reference path. Vehicle velocity v is 8 km $\cdot$ H^{-1}. As expected, during the straight line parts of the reference path (before curvilinear abscissa 30 m or after 55 m), the tracking error stays close to 0 (a 4 cm standard deviation from the mean can be computed). In contrast, during the curved part of the reference path, a significant lateral deviation appears and remains fairly constant (around 45 cm) all along the curve.

The same phenomenon occurs when tracking a straight line on a field with a constant slope. The lateral deviation recorded in such a situation is shown in Fig. 5: after a transient period, the vehicle suffers a lateral deviation of 30 cm. Some other experiments show that the asymptotic value depends on vehicle velocity, on the curvature of the reference path, and also on ground conditions.

2.2.4. *Influence of roll angle*

The tracking errors observed in Figs. 4 and 5 are indeed mainly due to sliding effects. To make this point clear, the contribution of roll angle in these errors is investigated here, and shown to be far less than the decimetre errors observed in these figures.

Some qualitative arguments are first presented. The GPS antenna is located on the top of the tractor cabin. This means

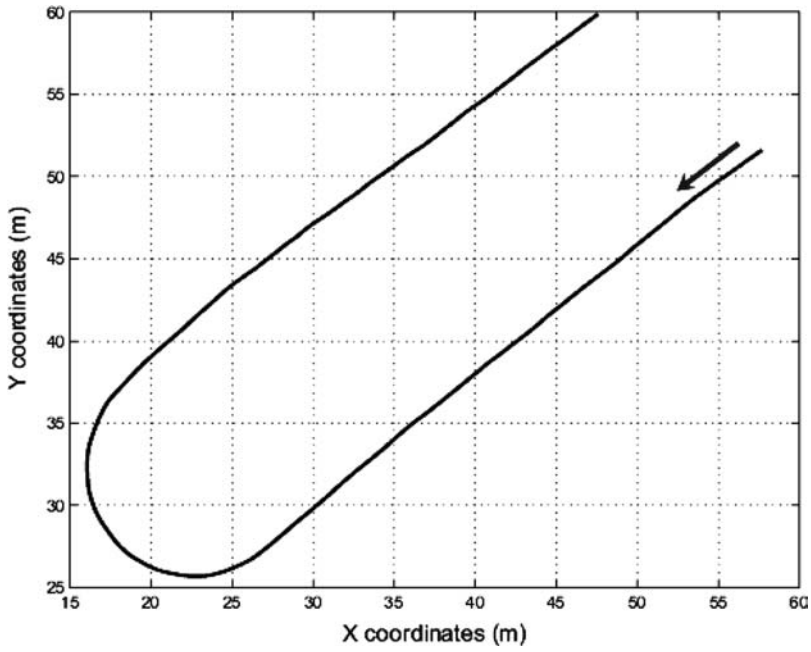

Fig. 3 Reference path

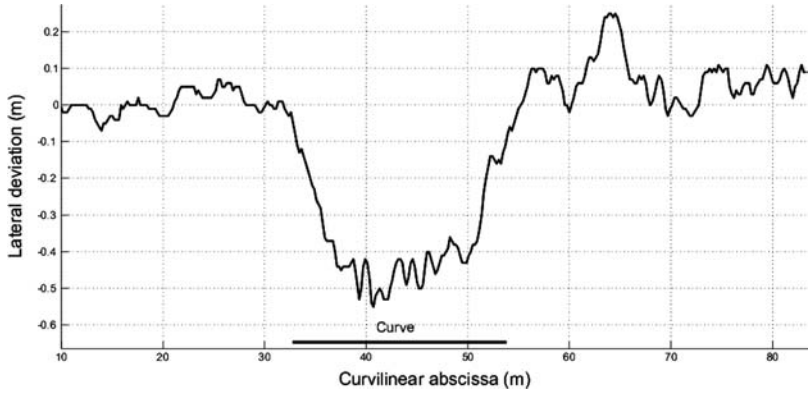

Fig. 4 Curved path tracking result, when relying on control law (4)

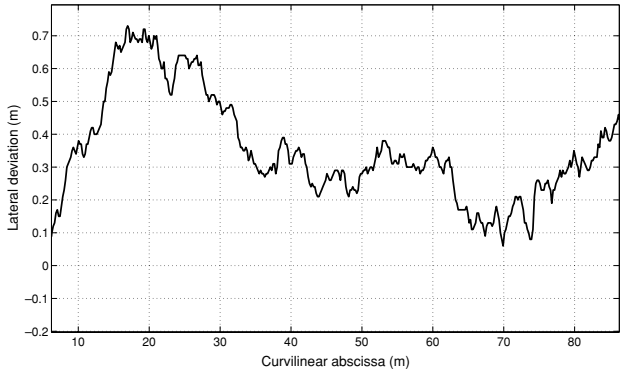

Fig. 5 Straight line following on a sloping field, relying on control law (4)

that the roll effect actually alters the absolute coordinates of the point O supplied by the RTK GPS sensor, and hence alters the vehicle lateral deviation thus recorded. Nevertheless, on level ground, the presence of the anti-roll bar ensures that the mean value of the roll angle is null, even when the tractor describes a curve. Therefore, the large tracking error observed in Fig. 4 cannot be explained by a roll effect. On sloping fields, the vehicle is of course inclined. However, when the reference path was recorded, the vehicle inclination was identical. In other words, the reference trajectory already includes the vehicle's inclination. Therefore, during automatic guidance on sloping fields, the roll effect introduces some noise in lateral deviation, but no bias. Once more, the large tracking error observed in Fig. 5 cannot be explained by a roll effect.

In order to provide quantitative arguments, the following experiment was performed. Two inclinometers were fitted to the vehicle, as shown in Fig. 6: one is located on the top of the tractor cabin (close to the GPS antenna) providing an angle that we shall call α_1. The other one is fitted on the rear axle (close to point O) and provides an angle that we shall call α_2. When the vehicle describes a curve, the rear axle is not inclined, and the measured angle α_2 records

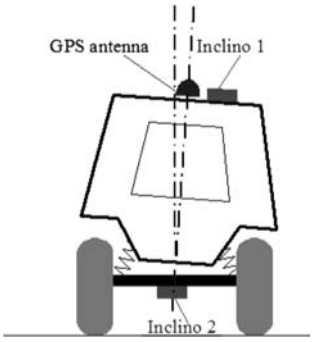

Fig. 6 Position of inclinometers

only the centrifugal acceleration (the inclinometers are mechanical ones and based on the measurement of the Earth's gravity). In contrast, the inclinometer located on the top of cabin measures both centrifugal acceleration and cabin inclination. Therefore, the cabin roll angle can be computed as the difference between the two angles supplied by the inclinometers. Finally the lateral deviation y_{inclino} induced by the roll angle is provided by relation (5) (where h is the cabin height, with $h = 3$ m):

$$y_{\text{inclino}} = h \sin(\alpha_1 - \alpha_2) \tag{5}$$

Figure 7 displays a comparison between the lateral deviation recorded by the RTK GPS sensor when the reference path shown in Fig. 3 is tracked, relying on control law (4) (already shown in Fig. 4), and the lateral deviation y_{inclino} computed according to relation (5).

It can be seen in Fig. 7 that there is no inclination of the cabin during the curve (deviation y_{inclino} stays close to 0), as was to be expected since the tractor is equipped with an anti-roll bar. There are only some transient inclinations at the beginning and at the end of the curve (at curvilinear abscissae 32 and 52 m). The 45 cm lateral deviation observed during the curve is therefore not due to a roll effect. In view of the amplitude of the signal y_{inclino}, the cabin oscillations can only provide the explanation for 10 cm. These oscillations are perceptible on the vehicle's lateral deviation, since this latter signal is actually corrupted by a 10 cm noise during the curve, greater than the 2 cm accuracy of the RTK GPS sensor.

3. Modelling with sliding incorporated

3.1. About dynamic modelling

Classically, the description of sliding relies on dynamic vehicle models, since kinematic ones are generally derived on the assumption of rolling without sliding.

First, inclusive dynamic models (e.g. see (Pham, 1986)) can be considered. These can describe vehicle dynamics as a whole, even when conditions of rolling without sliding are not satisfied. Only the classical dynamic parameters of the vehicle are required to run this kind of model (such as moments of inertia, position of centre of gravity, etc.). However, such models are designed on the assumption of tyre linearity: they are correct only in the case of pseudo-sliding (deformation of the tyre) and false as soon as tyre adherence is not ensured on the contact area with the ground.

For a complete description of sliding phenomena, general tyre models have to be considered. Such models, often used in the car industry (especially for trajectory control units such as ESP, see (Andréa-Novel et al., 2001) for example) are based on the celebrated Pacejka formula described in Bakker et al. (1987). Interaction forces on contact between the tyre and the ground depend on the one hand on variables (longitudinal slip, side slip angle, vertical load, camber, friction coefficient, etc.) to be measured (or estimated) on-line, and on the other hand on numerous empirical parameters (their number depends on the desired accuracy of the model) to be identified for each tyre.

Finally, these tyre models have to be coupled with a vehicle model. A complete description of vehicle dynamics thus requires (see, for instance (Thuilot, 1995) or (Dormegnie et al., 2002)) several sets of parameters:

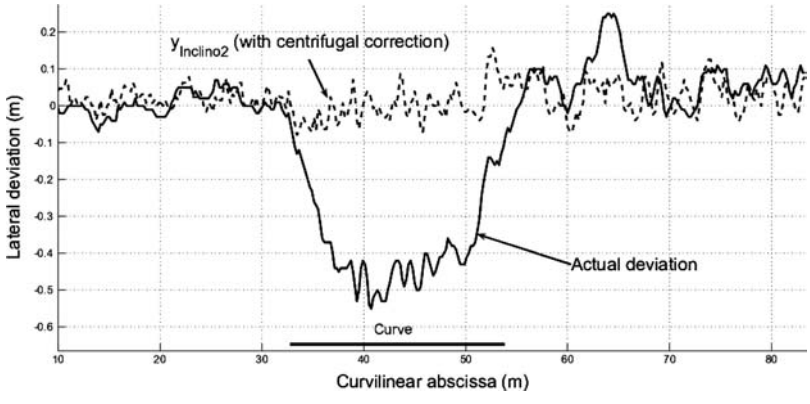

Fig. 7 Path tracking result compared to lateral deviation induced by roll angle

- Geometrical parameters: wheelbase, camber, position of gravity centre, etc.
- Inertial parameters: inertial moments or matrices, mass distribution on each tyre, etc.
- Vehicle state: longitudinal slip, side slip angle, etc.
- Tyre parameters (Pacejka empirical parameters for instance), which depend on tyre configuration (pressure, shape, etc.).

The use of such dynamic models is not convenient for agricultural vehicle guidance applications, since some of these numerous parameters and/or variables are very difficult to measure or to identify in an off-road context. Moreover, in agricultural tasks, some of these parameters can be expected to change as work progresses (e.g. tyre pressure, mass distribution and inertial moments if an implement is used, the coefficient of friction, which depends on both tyre and ground, etc.) so that measurements and/or identifications should be performed on-line, which is an additional difficulty. Therefore, in this paper, control design relying straightforwardly on such dynamic models is not considered. Dynamic considerations are investigated only with the aim of designing a kinematic model which could account for sliding effects. This new model will be referred to from now on as the "extended kinematic model".

3.2. The proposed modelling approach

As has been pointed out, a complete dynamic model does not appear tractable from a control design point of view, especially with respect to agricultural applications. However, in order to improve guidance accuracy in the presence of sliding, this latter phenomenon has to be taken into account in control laws, and therefore in vehicle modelling.

The proposed approach aims at preserving a kinematic structure. The sliding phenomenon is then introduced via its effects on vehicle motion: the additional movements due to sliding are described by parameters incorporated into a classical kinematic model derived on the assumption of rolling without sliding (such as model (1)). These parameters do not necessarily describe physical phenomena in detail, but are representative for the effects of these phenomena on vehicle motion. According to this approach, a complete description of the contact between the tyre and the ground is no longer necessary. With respect to dynamic models, the number of parameters to be measured or estimated is therefore considerably reduced. The kinematic structure of the proposed model, and the limited number of parameters to be measured/estimated are both very attractive features from a control design point of view.

In Lenain et al. (2003a), a first extended kinematic model was proposed to describe vehicle behaviour in the presence of sliding. This preliminary model is identical to a kinematic model designed under conditions of rolling without sliding, but two "sliding parameters" are additively incorporated into the equations describing the evolution of y and $\tilde{\theta}$. They are representative of the two motions induced by the sliding phenomenon (a pure lateral translation and a pure rotation). This approach, consisting in incorporating additive parameters to be estimated into a classical model, is inspired by nautical applications, where parameters are added to take into account the effect of current, see (Holzhüter and Schultze, 1996). Relying on this model, an adaptive control law based on Internal Model Control techniques has thus been designed (see (Thuilot et al., 2005) for further details). In this paper, another extended kinematic model is proposed, based on a partial dynamic analysis. This new model makes it possible to design an adaptive control law which is expected to be more reactive.

3.3. Extended kinematic modelling

The proposed extended kinematic model is derived from dynamic considerations relative to the interaction between the tyre and the ground. Specifically, when the assumption of rolling without sliding is satisfied, the direction of the velocity vector at the centre of the wheel remains in the wheel plane. This is no longer the case when sliding occurs, as shown in Fig. 8(a). The difference between the wheel plane and the actual direction of the velocity vector is called "side slip angle", and is denoted β_P in the sequel. This side slip angle is generated both by tyre

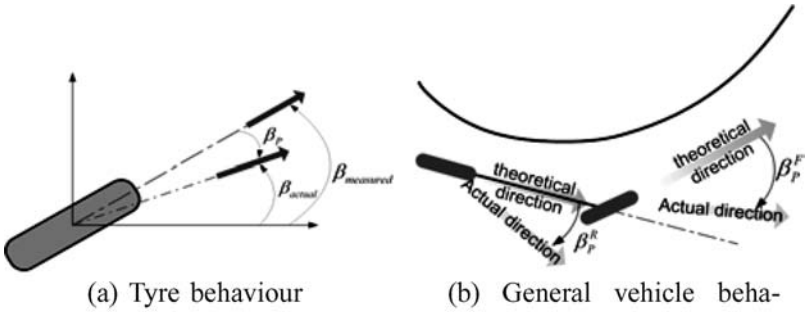

Fig. 8 Sliding parameters to be used in the extended kinematic model

(a) Tyre behaviour (b) General vehicle behaviour

deformation and by tyre slipping on the ground. It is the key parameter to describe the lateral component of the interaction force at the contact between the tyre and the ground, (see Bakker et al., 1987) or (Thuilot, 1995). From the dynamic point of view, this force ensures that the vehicle actually turns.

When a vehicle is described as a bicycle shape, such as in Fig. 2, two side slip angles β_P^F and β_P^R, associated respectively with the front and the rear virtual wheel, have to be considered, as shown in Fig. 8(b) . Tyre behaviour can then be introduced into the kinematic vehicle model according to the following analogy: the model of a car-like vehicle in the presence of sliding can be viewed as the model of a vehicle with two steerable wheels satisfying conditions of rolling without sliding. According to this view, the front steering angle is the addition of the actual steering angle and the front side slip angle, i.e. $\delta^F = \delta + \beta_P^F$, and the rear steering angle is directly equal to the rear side slip angle, i.e. $\delta^R = \beta_P^R$. Kinematic models of vehicles with two steerable wheels can be found for instance in Micaelli and Samson (1993). Replacing the steering angles δ^F and δ^R of such models according to this analogy leads to the desired extended kinematic model, describing car-like vehicle behaviour in the presence of sliding:

$$\begin{cases} \dot{s} = \dfrac{v\cos(\tilde{\theta} + \beta_P^R)}{1 - c(s)y} \\ \dot{y} = v\sin\left(\tilde{\theta} + \beta_P^R\right) \\ \dot{\tilde{\theta}} = v\left[\cos\beta_P^R \dfrac{\tan(\delta + \beta_P^F) - \tan\beta_P^R}{L} - \dfrac{c(s)\cos(\tilde{\theta} + \beta_P^R)}{1 - c(s)\,y}\right] \end{cases} \tag{6}$$

It can be checked that, as expected, the classical kinematic model for a vehicle in conditions of rolling without sliding can be recovered from (6): by applying null sliding parameters ($\beta_P^F = 0, \beta_P^R = 0$), the extended kinematic model (6) does indeed become identical to model (1).

4. Estimation of sliding parameters

As presented in Section 2.1, the only exteroceptive sensor on board is an RTK GPS unit. From the information supplied by this device, the whole vehicle state vector $(s, y, \tilde{\theta})$ can be inferred, so that control law (4), designed on the assumption of rolling without sliding, can actually be computed.

In order to account for sliding effects, control design has now to rely on the extended kinematic model (6). Hence, the sliding parameters β_P^F and β_P^R must also be supplied. These parameters are definitely not constant during the guidance task, since reference path curvature and adherence conditions are always varying. They cannot therefore be obtained via preliminary identification, but have to be measured or estimated on-line. Obviously, they cannot be directly supplied by the RTK GPS sensor. Moreover, accurate measurement of side slip angles does not appear realistic at limited cost. Therefore, the proposed approach consists in keeping the existing measurement device and then designing an estimation algorithm providing sliding parameters.

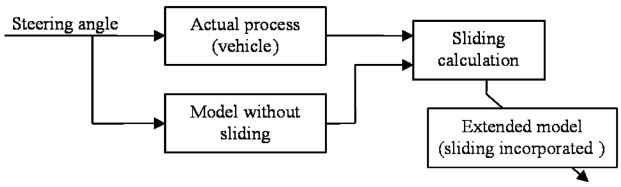

Fig. 9 Internal Model Adaptive Scheme

4.1. Estimation algorithm

The proposed estimation algorithm relies on the following hypothesis: the difference between the actual process (actual vehicle trajectory) and the model (1) designed on the assumption of rolling without sliding is solely due to sliding effects. As a consequence, sliding parameters can then be extracted via an Internal Model Adaptive scheme detailed in Lozano and Taoutaou, (2001), for example, or in Borne et al. (1990), and shown in Fig. 9: the desired steering angle (resulting from control law calculation) is entered into both actual process and model (1). The outputs of the process and the model are then compared to extract sliding parameter values.

4.2. Estimation design

Since the whole vehicle state vector $(s, y, \tilde{\theta})$ is directly measured, the derivative of these variables is available. Moreover, the steering angle δ can also be measured. As a consequence, all the variables appearing in the equations of the extended kinematic model (6) are available on-line, except the two sliding parameters to be estimated. These equations can therefore be solved to supply the desired sliding parameter values.

Since the vehicle's absolute heading θ is inferred from the RTK GPS sensor, the estimation algorithm can be slightly simplified by writing the vehicle model with respect to this latter variable, rather than with respect to the angular deviation $\tilde{\theta}$ (as it is done in model (6)). The equations to be inverted are indeed simpler:

$$\begin{cases} \dot{y} = v\sin\left(\tilde{\theta} + \beta_P^R\right) \\ \dot{\theta} = v\cos\beta_P^R \dfrac{\tan(\delta + \beta_P^F) - \tan\beta_P^R}{L} \end{cases} \tag{7}$$

Inverting Eq. (7) leads then to the following expression for the sliding parameters:

$$\begin{cases} \beta_P^R = \arcsin\left(\dfrac{\dot{y}}{v}\right) - \tilde{\theta} \\ \beta_P^F = \arctan\left(\dfrac{L\,\dot{\theta}}{v\cos\beta_P^R} + \tan\beta_P^R\right) - \delta \end{cases} \tag{8}$$

The relations (8) are not singular provided that:

- $v \neq 0$. This condition is always satisfied, since the vehicle's velocity is directly controlled by the operator (the farmer in agricultural applications).
- $|\dot{y}| < v$ (in order that the *arcsin* function in β_P^R expression may be properly defined. Moreover, it is assumed that the vehicle's velocity is always strictly positive). This condition reveals that the lateral deviation velocity has to be less than the overall vehicle velocity, which is the case in most of the situations encountered. Otherwise, this would mean that the vehicle is moving faster laterally than longitudinally. In such harsh situations, the vehicle is no longer steerable.
- $\beta_P^R \neq \frac{\pi}{2}[\pi]$. If this condition was not satisfied, then the direction of the velocity vector at the centre of the virtual rear wheel would be in the opposite direction from the direction defined by the wheel plane. Such a situation is never encountered in practical applications, since once more the vehicle would no longer be steerable.

However, the relations (8) cannot be used straightforwardly to provide sliding parameter values: since the RTK GPS device supplies only y and θ measurements, these quantities have to be numerically derived. The noise inevitably present on the measurements would then be significantly amplified by such a derivation, so that the resulting sliding parameter values would be very noisy. Filters therefore have to be introduced. They improve signal quality but slightly delay the estimation of sliding parameters. These limitations and potential improvements on the sliding estimation scheme are discussed below.

4.3. Validation of the extended kinematic model and of the associated estimation algorithm

4.3.1. Experimental validation

The first objective of the extended kinematic model is to describe vehicle behaviour in the presence of sliding with sufficient accuracy. This is an obvious preliminary point, in order to be able to design a new control law preserving guidance accuracy in the presence of sliding.

The capabilities of the extended kinematic model have been investigated as follows: in parallel to actual path tracking relying on control law (4), classical model (1) without sliding accounted and extended kinematic model (6) are both simulated. The measurements supplied to the vehicle by the RTK GPS sensor (vehicle state vector, actual vehicle velocity, etc.) are provided on-line to both simulators. In addition, sliding parameters β_P^F and β_P^R are provided to the extended kinematic model according to estimation algorithm (8). Of course, both simulations rely on the same control law (4) as the one actually used on the vehicle. Moreover, both simulators take into account the features of the steering actuator (identified as a second order process with a pure delay).

The actual path to be followed, shown in Fig. 3, was attempted on a level but wet field. It is composed of two straight lines linked by a half-turn. A sliding phenomenon mainly occurs when tracking the curved part of the trajectory. The lateral deviation y recorded during the actual path tracking is shown as a solid line in Fig. 10. It is compared to the lateral deviations provided by the simulations of classical model (1) (dashed line) and extended kinematic model (6) (dotted line).

Figure 10 can be separated into three parts:

- Straight line following (up to curvilinear abscissa 30 m). On level ground, even if the adherence properties are low, lateral behaviour is not perturbed by sliding effects, so that the lateral deviation y actually stays close to 0. Since sliding effects are not preponderant during this first part,

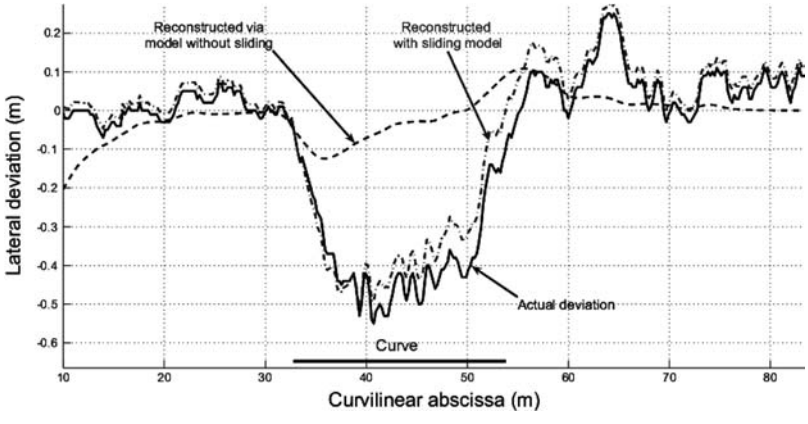

Fig. 10 Comparison between actual lateral deviation and simulations relying on models (1) and (6)

both simulator outputs are very close to the lateral deviations actually measured. This shows that classical control laws can achieve straight line following with satisfactory accuracy.

- Curve following (from 30 to 60 m). During this part of the trajectory, the vehicle turns, and consequently sliding occurs. Since control law (4) does not take such a phenomenon into account, the actual lateral deviation grows to 45 cm.

  More precisely, the lateral deviation simulated from classical model (1) stays close to 0 during this part. From the model (1) point of view, path tracking then appears satisfactorily achieved. Therefore, since control law (4) has been designed from this model, no steering action is generated in order to bring the vehicle back to the reference trajectory.

  On the contrary, the lateral deviation simulated from the extended kinematic model (6) fits the actual lateral deviation pretty well. This model therefore appears relevant to the design of a control law ensuring accurate path tracking in presence of sliding.
- Straight line following (after 60 m). When the reference trajectory turns into a straight line again, classical control (4) brings the vehicle back to the trajectory. Sliding effects are present only during the transient phase (from about 60 to 75 m), so that, after 75 m the lateral deviation has converged to 0.

Figure 10 demonstrates the relevancy of both extended kinematic model (6) and estimation algorithm (8) when sliding occurs during curve following. Sliding effects are however also observed when the vehicle is moving along a slope. In that case, the vehicle movement is more perturbed: since the vehicle is inclined, the behaviour of the shock absorbers is modified. In consequence, the oscillations of the tractor cabin with respect to the axle are amplified. Since the GPS antenna is located on the top of the tractor cabin, a disturbing lateral movement is thus generated. The estimated sliding parameters provided by relation (8) therefore have to be filtered.

Figure 11 shows the same results as Fig. 10 (with the same colour convention), when the reference path to be followed is a straight line on a field with a 15% slope. As usual in agricultural applications, this reference straight line is perpendicular to the slope. In such a configuration, gravity and low adherence properties on the field generate significant sliding effects.

The results observed in Fig. 11 are identical to those previously obtained during curve following. Due to the presence of sliding effects, the vehicle does not stay on the reference path: after a transient phase, the actual lateral deviation converges to around 30 cm. Nevertheless, from the model (1) point of view, path tracking is satisfactorily achieved: the lateral deviation thus simulated stays very close to 0 throughout straight line following. This explains why control law (4), designed from model (1), does not steer the vehicle back to the reference trajectory. However, it can satisfactorily be checked that the lateral deviation simulated from the extended kinematic model (6) fits once more with the actual lateral deviation. This demonstrates that this model, coupled with estimation algorithm (8), is also relevant to describing vehicle behaviour when sliding effects are induced by a slope.

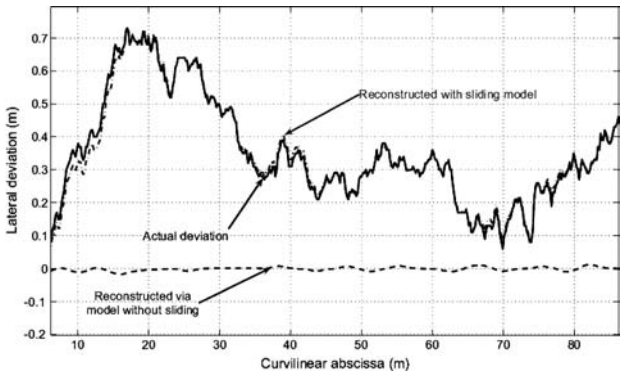

Fig. 11 Comparison between actual lateral deviation on a slope and simulation relying on models (1) and (6)

4.3.2. *Limitations of the estimation algorithm*

In the extended kinematic model (6), the 2 parameters β_P^F and β_P^R were introduced to account exclusively for sliding effects on the vehicle behaviour. However, they are estimated on-line by computing the difference between actual vehicle behaviour and the behaviour that can be expected when relying on the classical model (1) designed on the assumption of rolling without sliding, see relation (8). The sliding phenomenon is undoubtedly mainly responsible for this difference, but it is not the only factor. Consequently, sliding is not the sole phenomenon incorporated into the β_P^F and β_P^R values provided by estimation algorithm (8), contrary to initial expectations. Such an estimation strategy offers both advantages and drawbacks.

Positive effects: The sliding phenomenon is mainly responsible for the lateral deviations observed during path following. However, lateral deviations may also originate from dynamic phenomena (such as vehicle inertia, etc.) and delays (introduced for instance by the steering actuator). In view of the estimation algorithm (8), these phenomena are then also taken into account in the values of sliding parameters β_P^F and β_P^R and therefore integrated into model (6).

Thus the extended kinematic model (6) and the associated estimation algorithm (8) allow us to account not only for sliding effects, but also for several other phenomena, even if these are not explicitly described in the vehicle model. For example, this estimation strategy can compensate for bad

calibration of the right front wheel angular sensor used in the inner closed loop.

Negative effects: In view of the estimation algorithm (8), any phenomenon generating a lateral deviation is incorporated in the β_P^F and β_P^R values. Therefore, disturbances such as the noise on the measurements supplied by the RTK GPS sensor or ground irregularities (since they lead to cabin oscillations) are, alas, integrated into parameter estimation. The noise level on β_P^F and β_P^R is then unfortunately raised, but no bias is introduced. These negative effects can however be significantly reduced by the use of filters, as has already been mentioned.

As shown in Figs. 10 and 11, the extended kinematic model (6) and the associated estimation algorithm (8) can describe vehicle behaviour in actual agricultural applications with satisfactory accuracy (to a few centimetres), despite the occurrence of sliding. They therefore constitute relevant tools for designing high accuracy path tracking laws.

5. Control law design

As can be seen in Figs. 10 and 11, the classical control law (4), designed from model (1) constructed on the assumption of rolling without sliding, fails to provide satisfactory path tracking accuracy as soon as sliding occurs. When sliding conditions are constant, the lateral deviation also converges to a significatively large constant, e.g. 45 cm when performing the half-turn part of the reference path shown in Fig. 3 (see Fig. 10) or 30 cm when following a straight line on a 15% sloping field (see Fig. 11). In order to improve guidance accuracy in such situations, sliding effects must be taken into account explicitly in control law design. The extended kinematic model (6), as pointed out just above, reveals itself to be a relevant model to derive such a design.

5.1. Chained system transformation

In previous work (Lenain et al., 2003b), a complete adaptive control scheme was developed to steer a vehicle in the presence of sliding, relying on a slightly different extended kinematic model. In this paper, it is proposed to take advantage of the special structure of the extended kinematic model (6) in order to design a non-linear control law, providing better reactivity with respect to the phenomenon of liding.

As pointed out in Section 3.3, the extended kinematic model (6) is similar to the kinematic model of a vehicle with two steerable wheels, derived on the assumption of rolling without sliding. Such a model is known (e.g. see (Samson, 1995)) to be transformable into a form known as a chained system, from which relevant control laws can then easily be designed. More precisely, a 3-dimensional chained system is described by:

$$\begin{cases} \dot{a}_1 = m_1 \\ \dot{a}_2 = a_3 m_1 \\ \dot{a}_3 = m_2 \end{cases} \tag{9}$$

Such a chained form can actually be obtained from the extended kinematic model (6) by applying the invertible state transformation (10) and control transformation (11):

$$\begin{aligned} (a_1, a_2, a_3) &= \Theta(s, y, \tilde{\theta}) \\ &= (s, y, \tan\left(\tilde{\theta} + \beta_P^R\right)[1 - c(s)y]) \end{aligned} \tag{10}$$

$$(m_1, m_2) = M(v, \delta) \tag{11}$$

with the following definitions for m_1 and m_2:

$$m_1 = \frac{v \cos\left(\tilde{\theta} + \beta_P^R\right)}{1 - c(s)y} \tag{12}$$

$$m_2 = \frac{d}{dt}(\tan\left(\tilde{\theta} + \beta_P^R\right)[1 - c(s)y]) \tag{13}$$

The attractive feature of chained systems can be revealed by replacing time derivation by a derivation with respect to the first state variable a_1 (consistent here with s, the curvilinear abscissa). Provided that $m_1 \neq 0$ (which is true in view of definition (12)), chained system (9) is then turned, without any approximation, into a linear system:

$$\begin{cases} a_1' = 1 \\ a_2' = a_3 \\ a_3' = m_3 = \dfrac{m_2}{m_1} \end{cases} \tag{14}$$

where a_i' stands for $\frac{d\,a_i}{d\,s}$.

The only difficulty in this chained form conversion concerns control transformation (11): computation of m_2 according to (13) requires the derivation of rear sliding parameter β_P^R with respect to time. However, no analytical expression is available for β_P^R, and its value provided by the estimation algorithm (8) is too noisy to be numerically differentiated. Therefore, when deriving the expression for m_2 according to (13), β_P^R has been assumed to be a constant (i.e. $\frac{d}{dt}\beta_P^R = 0$), which finally leads to:

$$\begin{aligned} m_2 = &-c(s)v \sin\left(\tilde{\theta} + \beta_P^R\right) \tan\left(\tilde{\theta} + \beta_P^R\right) + v \frac{1 - c(s)y}{\cos^2\left(\tilde{\theta} + \beta_P^R\right)} \\ &\times \left[\cos\beta_P^R \left(\frac{\tan(\delta + \beta_P^F) - \tan\beta_P^R}{L}\right) - \frac{c(s)\cos\left(\tilde{\theta} + \beta_P^R\right)}{1 - c(s)y}\right] \end{aligned} \tag{15}$$

It can then be checked that state and control transformations (10–11) are invertible, provided that: $y \neq \frac{1}{c(s)}$ (singularity of model (6)), $v \neq 0$ (satisfied, since v is manually controlled by the driver) and $(\tilde{\theta} + \beta_P^R) \neq \frac{\pi}{2}[\pi]$ (satisfied when path tracking is properly initialized).

5.2. Control law design

Since extended kinematic model (6) can be converted, without any approximation, into a linear system (14), the design of a path tracking control law can now very easily be achieved.

Convergence of state variables a_2 and a_3 to 0 can easily be ensured by designing virtual control law m_3 according to:

$$m_3 = -K_d\, a_3 - K_p\, a_2 \ (K_p, K_d) \in \mathbb{R}^{+2} \tag{16}$$

since, by injecting (16) into system (14), the following equation for error dynamics is then obtained:

$$a_2'' + K_d\, a_2' + K_p\, a_2 = 0 \tag{17}$$

Differential Eq. (17) clearly implies the convergence of both variables a_2 and a_3 to 0. On one hand, in view of (10), the convergence of a_2 ensures the convergence of the lateral deviation y. The path tracking objective is therefore achieved. On the other hand, the convergence of a_3 implies that $(\tilde{\theta} + \beta_P^R) \to 0$. This means that vehicle heading compensates for rear sliding effects (the vehicle moves crabwise). Front sliding effects, as can be seen in the expression (18) below for the path tracking control law, are directly compensated by the steering angle δ.

The expression (16) of the virtual control law m_3 is consistent with a PD controller. Since the error Eq. (17) is written with respect to a_1 (which is equal to the curvilinear abscissa s), the gains (K_p, K_d) do not specify a settling time, but a settling distance. Thus the capabilities of the path tracking control law are theoretically independent of vehicle velocity v . From a practical point of view, the choice of (K_p, K_d) has nevertheless to take vehicle velocity into account in order to protect the steering angle sent to the actuator from saturation and from instabilities that would then be induced by the inner closed loop. However, if the gains are properly tuned, the capabilities of path tracking are actually velocity independent, as desired.

Finally, injecting (16) into (15) and (12), and inverting this relation, provides the non-linear analytic expression for the path tracking control law:

$$\delta = \arctan\left(\frac{L}{\cos\beta_P^R}\left[c(s)\frac{\cos\tilde{\theta}_2}{\alpha} + A\frac{\cos^3\tilde{\theta}_2}{\alpha^2}\right] + \tan\beta_P^R\right) - \beta_P^F \tag{18}$$

$$\text{with} \quad \begin{cases} \tilde{\theta}_2 = \tilde{\theta} + \beta_P^R \\ \alpha = 1 - c(s)y \\ A = -K_d\alpha\tan\tilde{\theta}_2 - K_p y + c(s)\alpha\tan^2\tilde{\theta}_2 \end{cases}$$

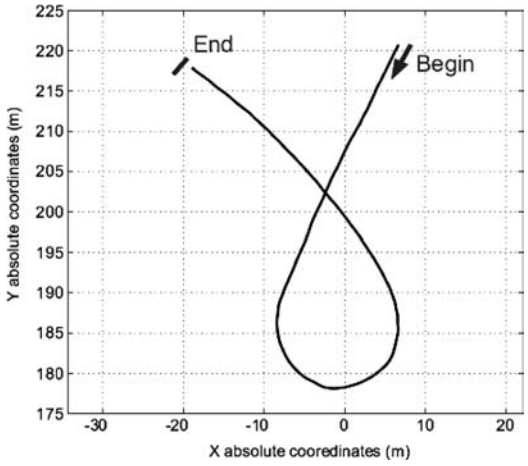

Fig. 12 Path #1: long constant curve on a level field

Relation (18) constitutes the steering angle value to be sent to the actuator. It can be checked that, as expected, the classical control law (4) designed on the assumption of rolling without sliding can be recovered from (18): by applying null sliding parameters $(\beta_P^F, \beta_P^R) = (0, 0)$, path tracking control law (18) becomes identical to control law (4).

5.3. Results without prediction

In order to investigate the performance and the limitations of the proposed approach, the new control law (18) was used to follow the path shown on Fig. 12. Sliding parameters β_P^F and β_P^R, required in control expression (18), are provided according to the estimation algorithm (8). Lateral deviation recorded during this experiment is shown as a dashed line in Fig. 13, and is compared with the deviation obtained when using the classical control law (4). In both cases, (K_p, K_d) were set to (0.09, 0.6), which corresponds to a 15 m settling distance.

Since it does not account for sliding effects, classical control law (4) leads to a constant tracking error during the curved part of the trajectory (in this case, the vehicle is 30 cm aside of the reference trajectory). On the contrary, the new control law (18) succeeds in bringing back the vehicle to the reference trajectory during the curve. Nevertheless,

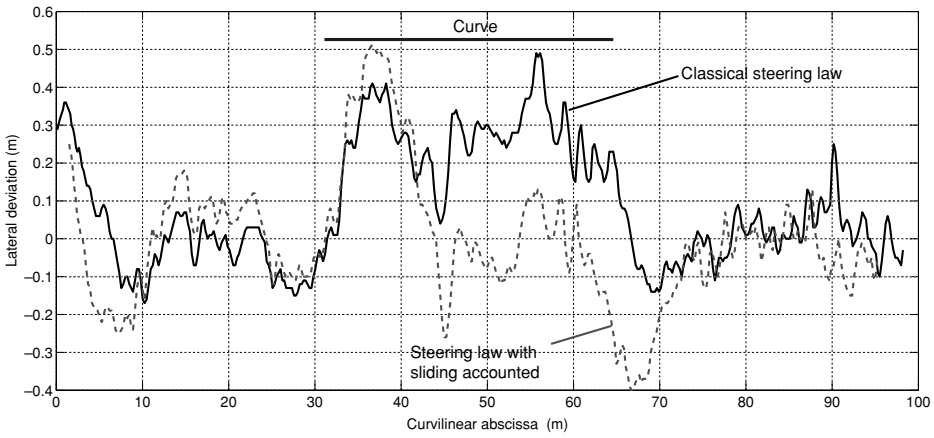

Fig. 13 Tracking error in curve following on a level field

transient errors still appear at the beginning and at the end of the curve, i.e. when the reference path presents a step in curvature. The delays introduced by the actuator features and vehicle inertia are responsible for such overshoots. This last difficulty is now addressed, relying on Model Predictive Control techniques.

5.4. Predictive control

Since, on one hand, the shape of the reference path is known in advance, and on the other hand, a model for the actuator response can be identified, predictive control can indeed be investigated. The objective is then to send a control value to the actuator a moment before the curve appears. Then, the steering angle actually applied to the vehicle when the curve starts could correspond to the desired angle and could prevent overshoots due to delays.

5.4.1. Separation of control law

Since angular and lateral deviations and especially sliding parameters cannot be anticipated, prediction has to be applied only with respect to curvature. To identify the contribution of curvature in control law (18), let us first assume that the vehicle follows the reference path perfectly. Considering this case and assuming conditions of rolling without sliding (since the values of sliding parameters cannot be predicted), the curvature defined by the vehicle's steering angle has to be equal to the curvature of the path. This condition can be mathematically described by:

$$\Rightarrow c(s) = \frac{\tan\delta}{L} \tag{19}$$

Condition (19) can be analytically checked: applying null deviations and sliding parameters to control law (18) leads to:

$$\delta(y=0,\tilde{\theta}=0)\big|_{\beta_P^R=0,\beta_P^F=0} = \arctan(L.c(s)) \tag{20}$$

These considerations show that the expression for the control law (18) can be split into two constituent parts:

$$\delta = \arctan(u+v) - \beta_P^F$$

$$\text{with} \begin{cases} u = \dfrac{L}{\cos\beta_P^R} c(s) \dfrac{\cos\tilde{\theta}_2}{\alpha} \\ v = \dfrac{L}{\cos\beta_P^R} A \dfrac{\cos^3\tilde{\theta}_2}{\alpha^2} + \tan\beta_P^R \end{cases} \tag{21}$$

which can be rewritten as the more convenient expression (22) using the geometrical relation (23):

$$\delta = \delta_{\text{Traj}} + \delta_{\text{Deviation}}$$

$$\begin{cases} \delta_{\text{Traj}} = \arctan(u) \\ \delta_{\text{Deviation}} = \arctan\left(\dfrac{v}{1+uv+u^2}\right) - \beta_P^F \end{cases} \tag{22}$$

$$\arctan(a+b) = \arctan(a) + \arctan\left(\frac{b}{1+ab+a^2}\right) \tag{23}$$

The expression of control law (18) in presentation (22) constitutes the desired separation of the control law into two additive terms, which play two different roles, as detailed below:

- $\delta_{\text{Deviation}}$: Null term when deviations and sliding are equal to zero. This term mainly depends on sliding parameters (β_P^R, β_P^F) and deviations $(y, \tilde{\theta}_2)$ to ensure the convergence of the latter to 0.
  As these variables and parameters cannot be anticipated, this additive term will not be introduced into the predictive algorithm.

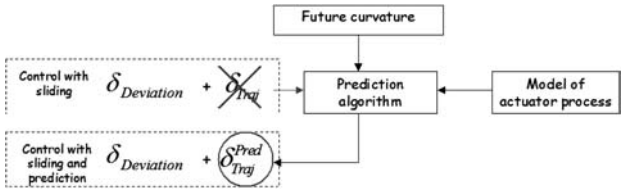

Fig. 14 Application of prediction to control expression

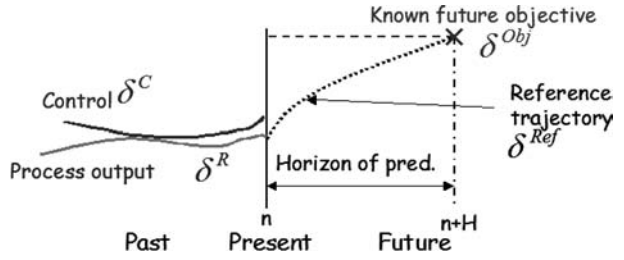

Fig. 15 Notations and general description of Model Predictive Control

- δ_{Traj}: Non-null term when deviations and sliding are equal to zero. This term mainly depends on the properties of the reference path, and ensures path-following conditions defined by (19).

  As the future curvature of the path to be followed is known (attached to the reference path), the future objective attached to this term can be calculated. This additive term will then be entered into the predictive algorithm.

The predictive control scheme is sketched in Fig. 14. The trajectory term δ_{Traj} is entered into the prediction algorithm (detailed below) and replaced by the output of this algorithm, named $\delta^{\text{Pred}}_{\text{Traj}}$. The new control law to be sent to the steering actuator is then the addition of $\delta_{\text{Deviation}}$ (which remains unchanged) and the predictive term $\delta^{\text{Pred}}_{\text{Traj}}$:

$$\delta = \delta^{\text{Pred}}_{\text{Traj}} + \delta_{\text{Deviation}} \tag{24}$$

5.4.2. *Prediction algorithm*

Since the future curvature is known and a model of the actuator is available, the Model Predictive Control principle, defined in Richalet (1993b) and applied in Richalet (1993a), is used to design the prediction algorithm. It requires the definition of the variables shown in Fig. 15 and detailed below:

- δ^C: Control variable sent to the actuator. In the current case of a separate control, this variable is only the trajectory part δ_{Traj} of the control law, defined by (21) and (22).
- δ^R: Measured steering angle. This is the output of low level process resulting from the action of control δ^C, which is only the trajectory part of the control actually applied.

As we cannot separate the measured steering angle into two parts, actual response to δ^C is approximated by the relation (25), where $\delta^M_{[n]}$ is the nth measurement of steering angle supplied by the sensor.

$$\delta^R_{[n]} = \delta^M_{[n]} - \delta_{\text{Deviation}[n]} \tag{25}$$

- H: Horizon of prediction. This is the constant time in the future, which will be used to determine the control value to be applied in the present (iteration n) to reach the future objective δ^{Obj} as well as possible. In the remainder of this paper, the integer n_H is the iteration number attached to the horizon of prediction H: n_H defines the number of coincidence points, i.e. $H = n_H T$ with T denoting the sampling period.
- δ^{Obj}: Known future objective. It represents the future desired process output value. In the present case, this variable is linked to the future curvature of the reference path by the relation: $\delta^{Obj} = \arctan(L.c(s + H_s))$, where H_s is the Horizon of prediction in the curvilinear abscissa associated with H.
- δ^{Ref}: Desired reference shape to be followed by the process output δ^R to converge to the future objective δ^{Obj}. Classically, a first order system is chosen. When successive objectives $\delta^{Obj}_{[i]}$ are considered on the prediction horizon, δ^{Ref} is defined by relation (26), where $i \in [0, n_H]$ and $\gamma \in [0, 1[$ is a parameter tuning the convergence speed of reference trajectory.

$$\delta^{Obj}_{[n+i]} - \delta^{Ref}_{[n+i]} = \gamma^i \left(\delta^{Obj}_{[n]} - \delta^R_{[n]}\right) \tag{26}$$

In the current case, only the objective at the moment n_H is used for reference path calculation and is considered as constant all along the horizon of prediction. The reference path is then defined as follows:

$$\delta^{Ref}_{[n+i]} = \delta^{Obj} - \gamma^i \left(\delta^{Obj} - \delta^R_{[n]}\right) \tag{27}$$

- $\hat{\delta}^R$: Predicted output of the process. This variable is the future response of the low level model (previously identified) to a given set of control δ^C.

Using these notations, the goal of Model Predictive Control is to find on the horizon of prediction H, the control set $\delta^C_{[n,\ldots,n+n_H]}$ which minimizes the deviation between predicted output $\hat{\delta}^R$ and the desired trajectory δ^{Ref} chosen to reach the objective δ^{Obj}. The first element of this set $\delta^C_{[n]}$ is then the term $\delta^{\text{Pred}}_{\text{Traj}}$ to be used in (24).

A criterion to be minimized can then be defined. It is shown graphically in Fig. 16, and the mathematical expression of this criterion, hereafter called D, is defined

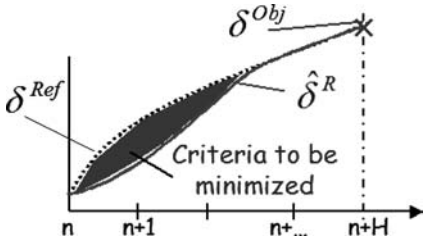

Fig. 16 Visualization of the criterion to be minimized

by:

$$D(n) = \Sigma_{i=0}^{n_H} \left(\hat{\delta}^{R}_{[n+i]} - \delta^{Ref}_{[n+i]}\right)^2 \tag{28}$$

In Eq. (28), the number of coincidence points used for criterion calculation, and consequently for minimization, is equal to the number of iterations required to meet the horizon of prediction. For example, if the horizon is set to 0.9 s, 10 iterations are required, and finally 10 coincidence points are defined.

5.4.3. Low level model and inertial compensation

As calculation of the criterion (and consequently its minimization) requires the prediction of the process output during the horizon of prediction, a model for the low level actuator must be available. Actuator response to some control inputs is then measured, and an identification establishes that the low level can be described as second order (with a 400 ms settling time and a 10% first overshoot). However, such an identification has been performed with no load on the steerable wheels. Actuator response may therefore be substantially different from that model in some of the experiments.

Moreover, the low level is not the only phenomenon generating overshoots. Vehicle inertia also plays a significant role during transient phases. The general equations of vehicle dynamics show that it is possible to account for such inertial effects by extending the low level model up to a third order system, see (Lenain, 2005). However, numerous parameters such as vehicle inertia, cornering stiffness, etc. would then have to be estimated. In agricultural applications, these parameters are very difficult to identify, and moreover they often vary in the course of the work. A more straightforward approach is therefore considered here: relying on the robustness of the predictive algorithm, its parameters (horizon of prediction H), and parameter γ introduced in the relation (27)) are empirically adjusted to take inertial effects into account as well as possible.

6. Experimental results

As demonstrated in Fig. 10, straight line following on a level field, whatever the adherence properties of the field

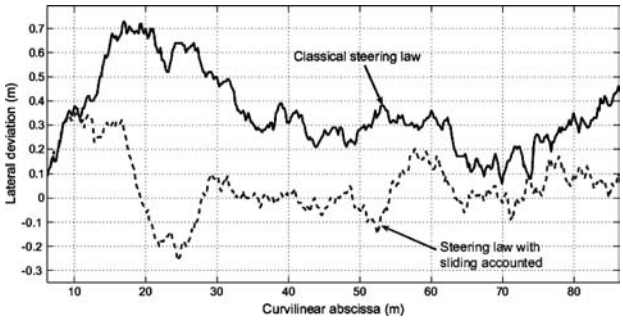

Fig. 17 Tracking error in straight line following in a sloping field

are, can be satisfactorily achieved either with classical control law (4), designed on the assumption of rolling without sliding, or with control laws (18) or (24), accounting for sliding effects, and relying on a prediction algorithm for the latter. The capabilities of control laws (18) and (24) are therefore investigated here with respect to guidance tasks where sliding effects actually occur and impair the tracking accuracy obtained when relying on classical control law (4).

The tracking errors obtained with the different control laws are compared in the figures shown below, where the colour convention is:

- solid line: tracking error when relying on classical control law (4), designed on the assumption of rolling without sliding.
- dashed line: tracking error when relying on control law (18), accounting for sliding effects.
- dotted line: tracking error when relying on control law (24), accounting for sliding effects and incorporating a prediction algorithm.

The reference paths were all recorded with the tractor manually driven, so that they are all clearly feasible (nonholonomic constraints are obviously satisfied). It should also be recalled that the maximum tracking accuracy that can be expected when vehicles are manually driven is ± 15 cm.

6.1. Straight line following on a sloping field

As already shown in Fig. 11 (and recalled in Fig. 17), classical control law (4) is not able to keep the vehicle on the reference path: after a transient phase, a 30 cm lateral deviation is recorded. In contrast, the lateral deviation recorded when relying on control law (18) is significantly reduced, and is very close to the accuracy obtained when the vehicles are manually driven. Control law (24) has not been considered since the reference path is a straight line, and therefore, no prediction can be made.

Figure 18 supplies statistical data on tracking error signals (mean, standard deviation and percentage of time inside the acceptance range of ± 15 cm). It can be clearly verified that control law (18) significantly improves the accuracy of

	Without sliding incorporated	With sliding incorporated
Mean	33 cm	4 cm
Std	18 cm	12 cm
In ±15 cm	9%	82%

Fig. 18 Deviation signal properties during straight line following on a sloping field

the tracking task (considering mean values or percentage of acceptance), and moreover reduces the maximum deviation recorded.

Path tracking along sloping fields is the worst case for automatic guidance systems. Even if the mean lateral deviation value is considerably reduced when using control law (18), it is not as close to zero as could have been expected having regard to theoretical results. The main reason is that the vehicle is moving crabwise (the orientation of the vehicle velocity vector is different from the vehicle heading). As a result, the vehicle heading, computed according to a Kalman filter based on the velocity measurements supplied by the RTK GPS sensor (see Section 2.2.2), is slightly biased, and therefore the guidance accuracy provided by control law (18) is also slightly impaired.

Moreover, on sloping fields, adherence conditions can quickly change. Due to the several filters used for practical reasons (essentially to deal with the cabin oscillations), such abrupt variations cannot be instantaneously taken into account by control law (18). Transient overshoots (such as at curvilinear abscissa 55 m on Fig. 17) can therefore be observed. Nevertheless, even in this difficult tracking application, the guidance capabilities of control law (18) (with respect to the mean and maximum lateral deviations recorded) are significantly superior to those obtained with classical control law (4).

6.2. Curved path following on level but slippery fields

The benefits of both sliding effects correction and the prediction algorithm are now investigated with respect to curved path following on level ground. Figures 19 and 22 present lateral deviations recorded when following path #1 and path #2 respectively. These reference paths are shown respectively in Figs. 12 and 21.

Path #1 is first considered. In Fig. 13, the relevancy of control law (18) has already been shown: during the curved part of path #1, the vehicle returns to the reference path while, on the contrary, a 30 cm lateral deviation is recorded when classical control law (4) is used. The only unsatisfactory result when relying on control law (18) is transient overshoots observed at the beginning and at the end of the curve, due to the delays introduced by the actuator features and vehicle inertia.

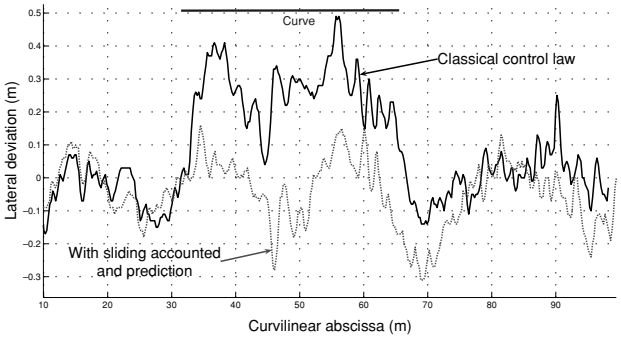

Fig. 19 Lateral deviation recorded while following path #1

	Without sliding incorporated	With sliding incorporated
Mean	16 cm	-5 cm
Std	17 cm	11 cm
In ±15 cm	8%	72%

Fig. 20 Deviation signal properties while following path #1

It can be seen in Fig. 19 that, as expected, the predictive algorithm incorporated into control law (24) succeeds in eliminating these overshoots, and still rejects sliding effects satisfactorily. The overall performance of the tracking task carried out is therefore improved: guidance accuracy remains satisfactorily within the target range ±15 cm (except at abscissa 48 m, where a hole is crossed).

Figure 20 presents the same statistical data as in 18, but with respect to the tracking of the curved part of path #1 (between curvilinear abscissa 30 to 80 m). It can be seen that control law (24) significantly improves the accuracy of the tracking task (the mean value and the percentage of acceptance could have been even more satisfactory without the negative overshoot at the end of the curve). Standard deviation is also improved and corresponds to the acceptance range of ±15 cm.

The tracking of path #2, shown in Fig. 21, is quite an arduous task since the curves to be followed are very close to each other. The tracking accuracy obtained when relying on control law (24), displayed in Figs. 22 and 23, appears

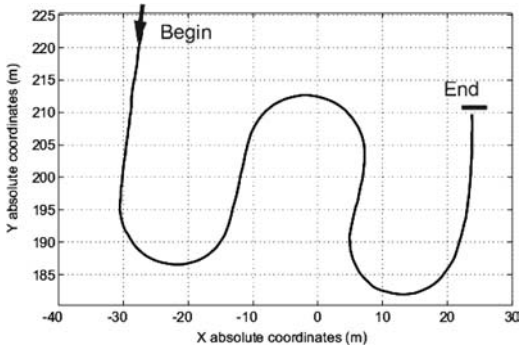

Fig. 21 Path #2: several half-turns on a level field

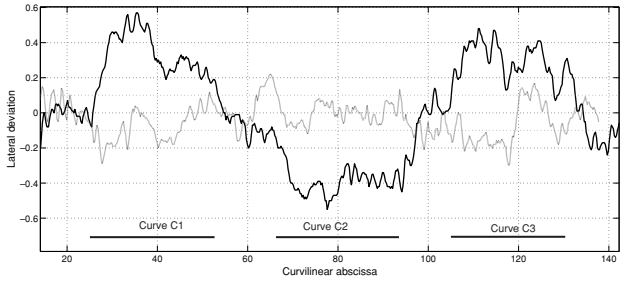

Fig. 22 Lateral deviation recorded while following path #2

	Without sliding incorporated	With sliding incorporated
Mean	4 cm	-3 cm
Std	30 cm	8 cm
In ± 15 cm	29%	90%

Fig. 23 Deviation signal properties while following path #2

very convincing: during 90% of the duration of the path following experiment, the tracking error remains in the target range ± 15 cm, while this same target range is reached for only 30% of the duration of the experiment when relying on the classical control law (4). Moreover, at curvilinear abscissae 25, 50, 65, 90, 105 and 130 m (i.e. at each important curvature variation) overshoots are not actually significant, as expected from the prediction algorithm. The mean values, displayed in Fig. 23, are not very significant here, because the lateral deviation is alternatively positive and negative, since the vehicle turns alternately to its right and to its left. Therefore, a small mean value, such as the value obtained with control law (4), does not imply that the tracking task is satisfactorily achieved, as can be verified in Fig. 22.

Finally, Fig. 24 compares the steering angle recorded when relying on control laws (4) and (24), while following path #1. First, it can be observed that the steering angle generated by control law (24) begins to grow earlier than the one generated by control law (4). This shows clearly the action of the predictive algorithm. Secondly, the steering angle applied to the vehicle appears to be smoothed when

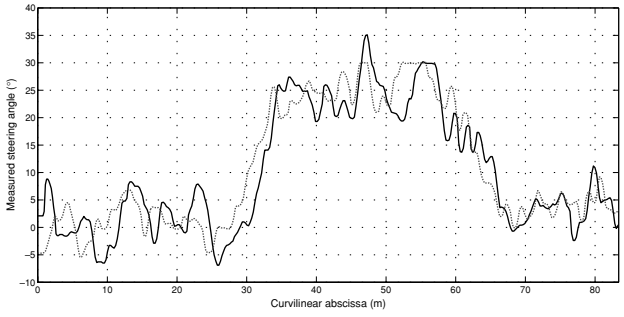

Fig. 24 Steering angle recorded while following of path #1

prediction is used. This improves comfort for passengers in the vehicle and reduces the stresses on vehicle mechanics.

The experimental results displayed in this Section show that the capabilities of control law (24) meet the expectations of agricultural applications, whatever the shape of path to be followed, and whatever the adherence conditions.

7. Conclusion and future work

7.1. A correction effective control law

The overall control algorithm presented in this paper proposes a high accuracy solution to achieve path-tracking for mobile robots in all-terrain conditions (independent of the shape of the path to be followed and of the adherence properties of the ground on which the vehicle runs). The main negative phenomenon compensated is sliding effects which are likely to occur in the agricultural applications considered here. Moreover, the proposed control algorithm can also compensate for the different delays due to low level actuators and vehicle inertial effects, which may be an important concern with heavy agricultural machines.

As the rolling without sliding assumption cannot be used, an extended kinematic model was designed, ensuring an accurate description of vehicle movement including lateral sliding effects, and preserving the advantage of the kinematic approach (the simplicity of such models, the possibility of measuring most of the required variables, etc.) The only two variables in this extended new model which cannot be directly measured are the sliding parameters.

These parameters are then estimated by comparing the vehicle's actual behaviour to the behaviour that can be expected from a vehicle model designed on the assumption of rolling without sliding. Disturbances due to other phenomena (such as pitch and roll motions due to vehicle mechanics and dynamic effects) can then lead to local misinterpretation. However, full-scale experiments have shown that this technique enables accurate reconstruction of the vehicle's behaviour in most of the situations encountered in practical cases.

The structural properties of the extended kinematic model were then used to designed a non-linear guidance law, relying on chained systems theory. The capabilities of such a control are satisfactory when sliding parameters vary slowly, but are limited by the inevitable delays due to both the steering angle actuator and vehicle inertia. As a result, overshoots appear as soon as a significant variation of curvature must be followed. Even if it only appears in isolation, such a phenomenon is not acceptable, as the tracking error recorded in such cases (e.g. when the vehicle is entering/leaving a curve) can reach quite significant values.

In order to prevent multiple overshoots in path tracking, a Model Predictive Control principle has been integrated into the proposed control law. Currently, as predictive control is indexed on the future curvature values of the reference path, benefits can be gained only during curved path tracking. The predictive principle is not yet transferred to slope anticipation, as there is no sensor measuring slope integrated into the process. Nevertheless, variations of sliding parameters induced by slope modifications are less abrupt than those generated by curvature changes.

Full scale experiments on tractors, in real working conditions (manoeuvring on fields typically used for agricultural production) highlight the benefits of the control laws with both sliding accounted and predictive action. The results presented in this paper show that tracking accuracy can be preserved whatever the path to be followed and whatever the adherence properties of the ground: the overall algorithm almost always keeps the tracking error within an acceptance range of ± 15 cm, with very limited variability, thus meeting the expectations of farmers.

7.2. Improvements and future work

The weakest part of the proposed control algorithm is currently the sliding estimation algorithm, especially on sloping fields, since vehicles are then moving "crabwise." The sliding estimation algorithm is a basic one, and can assuredly be improved. Observers (such as Luenberger, for example) are currently being developed to address this point. As a first step, such observers are expected to be applied only to the extended model and to rely solely on the current sensor system, i.e. the RTK-GPS device. As a second step, it is planned to test observers based on partial dynamic models, since the sliding parameters used in the extended kinematic model are compatible with such dynamic models. However, other sensors, such as a gyrometer, must then be used.

Dynamic models, even if they are not expected to be used specifically for control design (as explained at the beginning of this paper), can however be partially integrated into the overall control algorithm: either in the sliding estimation algorithm as mentioned above, or in order to improve the prediction algorithm. The model currently used for prediction does not take vehicle inertia into account, although such a dynamic effect implies delays when the vehicle has to turn. Such phenomena can be implicitly integrated into the prediction algorithm by tuning the horizon of prediction, as is done in this paper. However, the efficiency of the prediction algorithm can be improved by considering explicitly simplified dynamic models. Such simplified dynamic modelling is currently under study.

Finally, the control algorithm presented in this paper relies exclusively on a single RTK-GPS sensor. Disturbances due to the position of the antenna, which is very sensitive to pitch and roll movements, can be misinterpreted by the estimation algorithm (although it can be improved by observation techniques) and consequently by the control law, thus impairing path following accuracy. Future work will therefore also deal with the addition of sensors to increase the accuracy of estimation of sliding parameters.

References

Andrea-Novel, B.d'., Chou, H., Ellouze M., and Pengov, M. 2001. An optimal control strategy for a vehicle to brake in corner with stability. In *Journees Automatique et Automobile,* Bordeaux, France.

Bakker, E., Nyborg, L., and Pacejka, H.B. 1987. Tyre modeling for use in vehicle dynamics studies. In *International Conference of the Society of Automotive Engineers* (*SAE*), Warrendale USA, pp. 2190–2204.

Borne, P., Dauphin-Tanguy, G., Rotella, F., and Zambettakis, I. 1990. *Commande et optimisation de processus*. Methodes et pratiques de 1'inge-nieur. TECHNIP Editions. Paris, France.

Brunnert, A. 2003. Machine guidance with laser and GPS. In *Conference on Crop Harvesting and Processing*. Kentucky, USA.

Cordesses, L. 2001. Commande de robots: applications a 1'asservissement visuel 3D et au guidage d'engins agricoles par GPS. PhD thesis. Universite Blaise Pascal -Clermont-Ferrand, France.

Debain, C., Chateau, T., Berducat, M., Bonton, P., and Martinet, P. 2000. A guidance system for agricultural vehicles. *Computers and Electronics in Agriculture*, 25(1/2):29–51.

Dormegnie, E., Fandard, G., Mahajoub, G., and Zarka, F. 2002. Dynamique du vehicule. Technical report. IFMA. Clermont-Ferrand France.

Ellouze, M. and Andréa-Novel, B.d'. 2000. Control of unicycle-type robots in the presence of sliding effects with only absolute longitudinal and yaw velocities measurement. *European Journal of Control*, 6(6):567–584.

Holzhüter, T. and Schultze, R. 1996. Operating experience with a high precision track controller for commercial ships. *Control Engineering Practice*, 4(3):343–350.

Lenain, R. 2005. Contribution à la modélisation et à la commande de robots mobiles en présence de glissement. PhD thesis. Université Blaise Pascal Clermont-Ferrand II (France).

Lenain, R., Thuilot, B., Cariou, C., and Martinet, P. 2003a. Adaptive control for car like vehicles guidance relying on RTK GPS: Rejection of sliding effects in agricultural applications. In *IEEE International Conference on Robotics and Automation*. Taipei (Taiwan), Vol. 1. pp. 115–120.

Lenain, R., Thuilot, B., Cariou, C., and Martinet, P. 2003b. Rejection of sliding effects in car like robot control: Application to farm vehicle guidance using a single RTK GPS sensor. In *IEEE/RSJ International Conference on Intelligent Robots and Systems*. Las Vegas (USA), Vol. 4. pp. 3811–3816.

Lindgren, D.R., Hague, T., Probert-Smith, P.J., and Marchant, J.A. 2002. Relating torque and slip in an odometric model for an autonomous agricultural vehicle. *Autonomous Robots*, 13(1):73–86.

Lozano, R. and Taoutaou, D. 2001. *Identification et commande adaptative,* Hermes, Paris, France.

Micaelli, A. and Samson, C. 1993. Trajectory tracking for unicycle-type and two-steering-wheels mobile robots. Technical Report 2097. INRIA. Sophia-Antipolis France.

Nagasaka, Y., Otani, R., Shigeta, K., and Taniwaki, K. 1997. Automated operation in paddy fields with a fiber optic gyro sensor and GPS.

In *International Workshop on Robotics and Automated Machinery for Bio-Production* B*io-Robotics*, Valencia, Spain, pp. 21–26.

O'Connor, M., Elkaim, G., Bell, T., and Parkinson, B. 1996. Automatic steering of a farm vehicle using GPS. In *International Conference on precision agriculture,* Mineapolis, USA, pp. 767–777.

Pham, M. 1986. Modélidation mathématique du comportement dynamique d'une automobile dans le domaine non-linéaire. *Revue de la Société des Ingénieurs Automobile*. Vol. 40.

Reid, J. and Niebuhr D. 2001. Driverless tractors. *Ressource*, 8(9):7–8.

Richalet, J. 1993a. Industrial applications of model based predictive control. *Automatica*, 29(5):1251–1274.

Richalet, J. 1993b. *Pratique de la commande predictive.* Traite des nouvelles technologies, sèrie automatique, Hermes, Paris, France.

Samson, C. 1995. Control of chained system. *IEEE Transaction on Automatic Control*, 40:64–77.

Thuilot, B. 1995. Contribution à la modelisation et à la commande de robots mobiles à roues. PhD thesis. Ecole Nationale Supérieure des Mines de Paris (France).

Thuilot, B. Cariou, C., Martinet, P., and Berducat, M. 2002. Automatic guidance of a farm vehicle relying on a single CP-GPS. *Autonomous Robots*, 13(2):53–71.

Thuilot, B., Lenain, R., Martinet, P., and Cariou, C. 2005. Accurate GPS-based guidance of agricultural vehicles operating on slippery grounds. In J.X. Liu (ed.), *Focus on Robotics and Intelligent Systems Research* . Nova Science publisher USA.

Roland Lenain is a research engineer in Cemagref on the topic of agriculture robotics. His research interests include the modeling and the control of agricultural vehicles. The aims of research are the development of automatic devices for farmer comfort, environmental aspects and safety. He was graduated from IFMA (French Institute for Advanced Mechanics) in 2002. He received is Ph.D. degree in Robotics from the Blaise Pascal University in 2005.

Benoit Thuilot received his Electrical Engineer and PhD Diploma in 1991 and 1995. He held postdoctoral appointment at INRIA research units of Grenoble, France (1996) and of Sophia-Antipolis, France (1997). Since 1997, he is an assistant professor at Blaise Pascal University of Clermont-Ferrand, France. He is also a research scientist at LASMEA-CNRS Laboratory - Clermont-Ferrand. His research interests include nonlinear control of mechanical systems, with application to automatic guided vehicles. Intelligent Transportation Systems and Off-Road vehicles are both addressed.

Christophe Cariou received his Electrical Engineer Diploma from CUST, University of Clermont-Ferrand, France, in 1994. He spent three years in the Electrical industry. Since 1998, he has been working on automatic guided farm vehicles at Cemagref, Clermont-Ferrand.

Philippe Martinet graduated from the CUST, Clermont- Ferrand, France, in 1985 and received the Ph.D. degree in electronics science from the Blaise Pascal University, Clermont-Ferrand, France, in 1987. Since 2000, he has been a Professor with Institut Français de Mécanique Avancée (IFMA), Clermont-Ferrand. He is performing research at the Robotics and Vision Group of LASMEA-CNRS, Clermont-Ferrand. He is the leader of the group. His research interests include visual servoing, vision-based control, robust control, automatic guided vehicles, enhanced mobility, active vision and sensor integration, visual tracking, and parallel architecture for visual servoing applications.